Procedia Manufacturing

Volume 5, 2016, Pages 1018–1030

44th Proceedings of the North American Manufacturing Research Institution of SME http://www.sme.org/namrc

A Novel Method for Additive/Subtractive Hybrid Manufacturing of Metallic Parts

Wei Du[1], Qian Bai[1], Bi Zhang[1,2]

[1] *Key Laboratory for Precision and Non-traditional Machining Technology of Ministry of Education, Dalian University of Technology, Dalian, China.*

[2] *Department of Mechanical Engineering, University of Connecticut, Storrs, USA.*
duwei_8848@mail.dlut.edu.cn, baiqian@dlut.edu.cn, zhang@engr.uconn.edu

Abstract
Additive Manufacturing (AM) has been developed for industrial applications due to its superior capabilities, such as building complicated parts that are otherwise difficult to manufacture by the conventional methods. However, the dimensional and geometric accuracies as well as surface quality of an AM produced part are inferior to the conventionally machined part, which hinders the AM applications. A novel additive/subtractive hybrid manufacturing (A/SM) method is developed to take advantage of both simplex AM and precision milling. The method combines the selective laser melting with precision milling for improved surface finish as well as geometric and dimensional accuracies of a part. This study presents the research outcomes of A/SM of an 18Ni maraging steel part, analyzes its microstructure and hardness variations, and compares it with those made by the simplex AM and other methods. The study also deals with material characterization with X Ray Fluorescence (XRF), X-ray diffractometry (XRD), scanning electron microscopy (SEM), and hardness measurement. The study provides a valuable guide for determining the A/SM process parameters.

Keywords: *Additive/Subtractive Hybrid Manufacturing; 18Ni Maraging Steel; Microstructure; Hardness*

1 Introduction

Additive Manufacturing (AM) offers great advantages of building parts with geometric and material complexities. For metallic materials, the AM methods include selective laser melting (SLM) (Rombouts et al., 2006), selective laser sintering (SLS) (Khaing et al., 2001), fused deposition modelling (FDM) (Masood, 1996), laser-engineered net shaping (LENS) (Griffith et al., 1996), directed light fabrication (DLF) (Lewis et al., 1997) and electron beam melting (EBM) (Murr et al., 2012), etc. However, the AM methods provide a relatively poor surface finish and quality, as well as dimensional and geometric accuracies.

 Selection and peer-review under responsibility of the Scientific Programme Committee of NAMRI/SME

doi:10.1016/j.promfg.2016.08.067

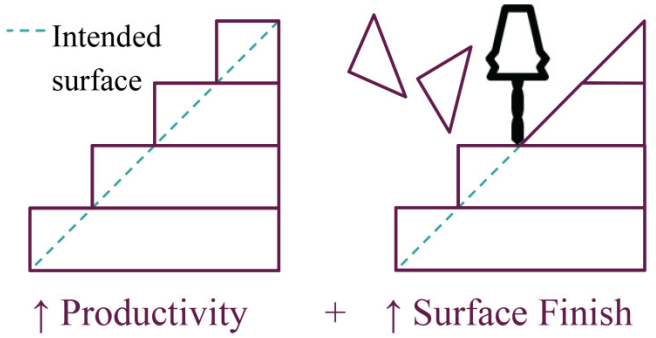

Figure 1: Cross-sectional view showing how an overbuilt part is machined using the combination of AM and machining (Lorenz et al., 2015).

In order to eliminate the 'stair effect' shown in Figure 1, the shape deposition manufacturing (SDM) (Fessler et al., 1996) and controlled metal build-up (CMB) (Freyer et al., 2001) used a combination of additive and subtractive techniques to accomplish the deposition and the machining processes in the same setup (Song et al., 2005). In these methods, powder material was sprayed through a nozzle into the spot of a laser beam focused on the workpiece, and the relative inaccuracy of the powder jet deposition was remedied by applying a CNC milling operation that milled the contour and the upper surface of each layer before applying the next one (Kruth et al., 1998). These methods propose frameworks for applying the concept of additive/subtractive hybrid manufacturing.

Other research work on hybrid processes has been done such as 3D welding and milling for fabrication of metallic prototypes (Song et al., 2005) and the hybrid plasma deposition and milling for aero-engine components (Xiong et al., 2010). Additionally, selective laser cladding (SLC) and milling was combined for mold fabrication and modification (Jeng et al., 2001). Similarly, CO_2 laser welding were combined with conventional milling for rapid prototyping and tooling (Choi et al., 2001). Recently, a CNC milling machine was integrated with an arc welding unit (Karunakaran et al., 2010). A study was also conducted on the machinability of materials fabricated by a hybrid process (Aziz et al., 2012).

Distinctive advantages can be provided by combining the SLM as an additive and milling as a subtractive process over the conventional machining and simplex AM. Firstly, if a large volume must be removed, a competitive approach can be offered in terms of fabrication time by using the additive method and subsequent surface finishing during the fabrication of a near-net-shaped part. In addition, if the material is a rare metal or difficult-to-machine material, the near-net-shaped part offers an economic way for the subtractive process because of less machining chip waste and tool wear. Secondly, some special features that are either impossible or difficult to machine can be manufactured using the hybrid method, such as a hollow structure or internally conformal cooling channel. Thirdly, the combined process permits fabricating accurate parts with various materials, depending on the functional requirements (Song et al., 2005). Fourthly, it is believed that the part produced by A/SM presents higher fatigue strength than that produced by the simplex AM process because of the difference in surface quality (Kasperovich et al., 2015).

Maraging steels with a low carbon content combine good mechanical properties, e.g. yield and tensile strengths with toughness and weldability. This combination of properties is attributed to the microstructure consisting of the fine intermetallic structure in the cubic martensitic matrix compounds obtained by heat treatment.

Maraging steels are well suited for the A/SM process for three reasons. Firstly, the material with the martensitic matrix needs to be quenched rapidly to a temperature that converts austenite to martensite. Because of the relatively small size of the melt pool in the A/SM process, cooling time is typically short so as to easily obtain the martensitic structure. Secondly, while the steel is still in the

condition after the additive laser process and before age-hardening, machinability is excellent becaXuse of the low hardness of the materials. After the whole A/SM hybrid process, a proper heat treatment can be conducted with little dimensional variations. Thirdly, maraging steels are mainly used in the aerospace industry and tooling applications due to their substantially high cost. These industries often require geometrically complex components with excellent external and internal surface quality in a small batch, which can be achieved by the A/SM process (Jägle et al., 2014).

In this study, a novel method is proposed for hybrid additive/subtractive manufacturing of metallic parts, such as maraging steel parts. The method combines an SLM system with a CNC milling machine. The study focuses on the method of producing a metallic part with curved cooling channels, and the characterization of the part material.

2 Process of additive/subtractive hybrid manufacturing

A schematic description of the A/SM process is shown in Figure 2. A digital CAD model is divided into thin slices which are then virtually constructed by the selective laser melting method layer by layer. A substrate is clamped onto the worktable as shown in Figure 2. The part is built from powders as the laser beam scans across the surface of the powder bed and causes the powders to melt. After a layer is sintered, the build platform lowers by one layer and receives a new layer of powders on top of the sintered layer. This new layer is melted and the process repeats for several times, then a milling cutter comes to machine the part being built. Following the milling process is the next additive process for the successive several layers. The additive and subtractive processes occur alternatively until the part is finished. In the A/SM process, complex internal structures, such as cooling water channels, can be formed and machined. Moreover, the dimensional and geometric errors from the additive process can be corrected by the milling process.

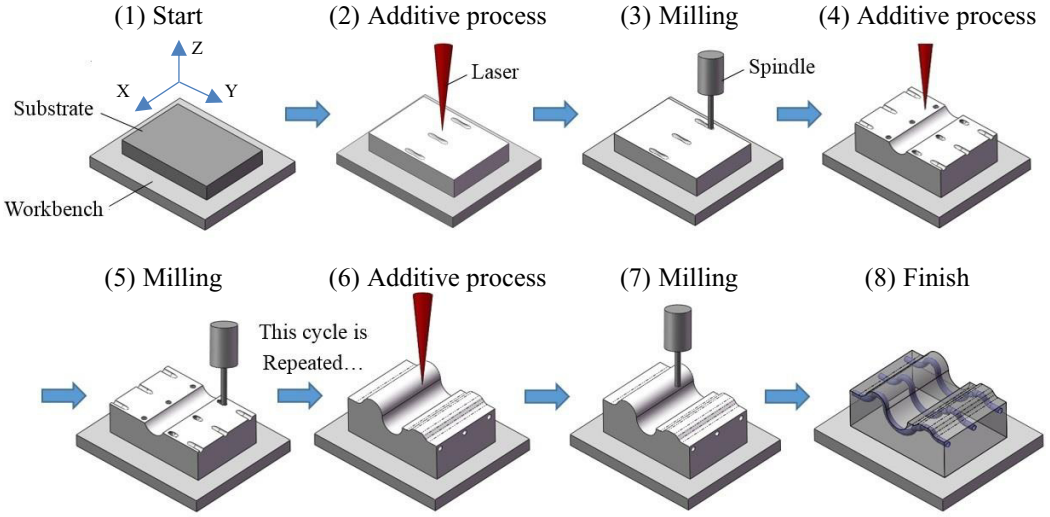

Figure 2: Schematic description of the hybrid A/SM process.

3 Experimental procedures

The experimental study was performed on an additive and subtractive machine (Sodick OPM250L shown in Figure 3). The machine was equipped with a 500 W fiber laser with a wavelength of 1070 nm and an adjustable beam diameter depending on location of the laser beam in the Z direction. It combined the additive SLM and subtractive high speed milling processes. The powder bed could travel 250 mm in the Z direction. The CNC milling machine could travel for 260 mm in the X, Y directions and 100 mm in Z direction. The maximum spindle speed was 45,000 rpm, and the maximum torque of the spindle was 0.8 N·m. The automatic tool changing system was able to pick up the appropriate cutting tool from the tool magazine which accommodated 16 sets of different tools.

The working chamber had a 290×290×260 mm workspace, and was vacuumed and then filled with nitrogen gas at a pressure of 10 mbar to protect a part being fabricated. The protective atmosphere allowed preventing the oxidation during the fabrication process by maintaining the oxygen content below 0.2%.

Figure 3: Additive and subtractive hybrid machine (Sodick OPM250L).

3.1 Hybrid process parameters

This study used 18Ni (C300) maraging steel powders that were supplied by Sodick Co. Ltd. The powders followed the Gaussian distribution in terms of the particle size with a mean value of 35 μm. Figure 4 (a) shows a schematic of an injection mold sample with multiple internal flow channels. Similar to the process shown in Figure 1, the internal channels were machined by the milling process during the laser additive process.

The microstructure evolution of an A/SM part mainly depended on the local heat transfer condition which was influenced by laser energy, scanning speed, heat conductivity of the powder bed, etc. The additive process parameters were determined based on the considerations of the mold sample quality. The layer thickness was constantly 40 μm. The laser machine was operated at a power of 420 W and the laser beam travelled at a speed of 1400 mm/s with a 0.2 mm spot diameter.

A stainless steel plate with dimensions of 125 mm × 125 mm × 15 mm was used as a substrate. Before being clamped onto the worktable, the substrate was blasted with alumina. The 'Island' scanning strategy was applied in order to decrease residual stresses of the mold sample: each layer of the powders was divided into small islands that were raster scanned with short scan tracks in a random order, as illustrated in Figure 5. The scanning directions in the neighboring islands were perpendicular to each other. In the subsequent layer, the islands were shifted by 1 mm in both the X and Y directions. The island scanning strategy can effectively decrease the distortion and cracking problem (Kruth et al., 2004).

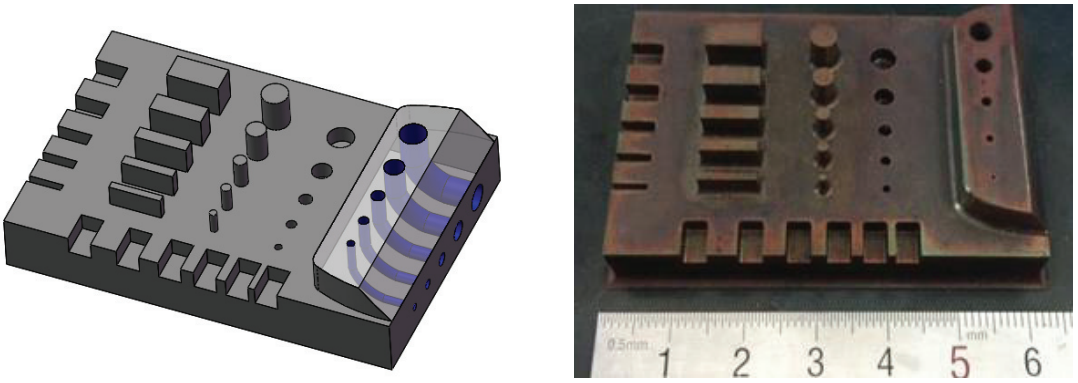

(a) 3D view of the mold sample (b) Photographic view of the mold sample

Figure 4: (a) Schematic of an injection mold sample with internal cooling channels and (b) the mold sample fabricated by the A/SM hybrid process and heat treatment.

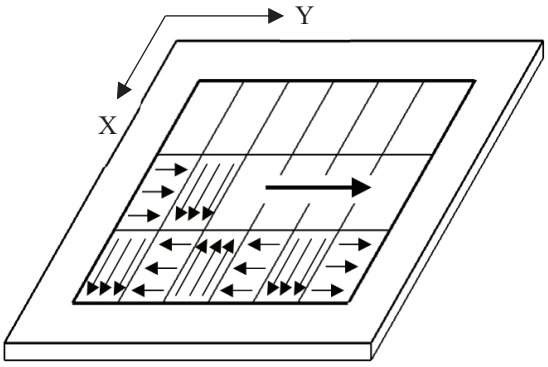

Figure 5: Laser scanning strategy used in the A/SM experiment.

The milling tool intervened every ten constructed layers to finish the contour of the new layers and the surface of the sample. During the subtractive process two milling cutters were used according to the different needs for machining, one with a diameter of 2.0 mm, and the other with a diameter of 1.0 mm. The cutting tool was not interfered by the powders due to good flowability.

Due to the molten pool in the SLM process, the workpiece temperature is relatively high for high speed milling. However, different from the traditional cutting processes, liquid coolant is prohibited in the A/SM process since it may have an adverse effect on the powder bed. In A/SM due to the tool changing process, there is a time interval between the SLM and milling processes, heat transfer takes

place in the time interval, leading to a temperature drop in the workpiece. Nevertheless, the workpiece temperature is still higher than that in the traditional cutting, which may cause rapid tool wear in A/SM. How to optimize this time interval to suppress tool wear needs further investigation.

Maraging steel has a relatively low thermal expansion coefficient, and thus its geometric accuracy is temperature-insensitive under the condition of an elevated temperature in A/SM. Since AM is a near-net-shaped process, only a minimal amount of material removal is required for the A/SM workpiece. Therefore, the cutting chips are relatively small in size compared to that in the traditional cutting processes, and should not have a significant effect on the next powders layer.

After the A/SM hybrid process, the sample was heat treated. The heat treatment process was arranged for three hours at 500 °C in a vertical tube furnace and cooled down naturally in the furnace.

3.2 Material characterization and properties

After the A/SM and heat treatment, X-Ray Fluorescence (XRF) was used to determine the chemical compositions of the A/SM fabricated mold sample. X-Ray diffractometry (XRD) with a Rigaku D/MAX Ultima plus diffractometer was used to determine the crystal structure and phase compositions of the sample, for which $CuK\alpha_1$ radiation was used. Reflections in the 2θ range of 40–80° were recorded.

Cross-sectional surfaces perpendicular and parallel to the building direction were observed. For the purpose of observations, samples were polished using an SiC sand paper of a fine #2000 mesh size, and an SiO_2–H_2O_2 solution. To reveal microstructure of the sample, the polished surfaces were etched in a mixture of 100 ml anhydrous alcohol and 3 ml nitric acid. The study was performed on an FEI ULTRA55 scanning electron microscope (SEM) to evaluate the microstructure of the A/SM sample in different directions and locations, and then the microstructure with that of the simplex SLM and argon induction melting (AIM) casting samples was compared.

Rockwell hardness tests were performed by using an automated CLEMEX® hardness tester. The tests were conducted on the surface of the sample in different directions and locations. Before the tests, the sample was polished in order to remove the oxide layer in the surface generated during the heat treatment. For each location, 10 measurements were conducted and the mean value of the measurements were calculated. The relative density was measured by the Archimedes method in a deionized water according to the ASTM B311-13 standard.

4 Results and discussion

Figure 4 (b) shows the mold sample with the cooling channels produced by the A/SM and heat treatment processes. The chemical compositions (wt%) of the A/SM sample are given in Table 1 and compared with the nominal maraging steel, grade 300.

	Fe	Ni	Co	Mo	Ti	Cr
A/SM	65.07	17.75	8.89	4.90	0.73	0.09
Nominal (Cubberly et al,.1979)	Rem.	17-19	8.5-9.5	4.5-5.2	0.6-0.8	<0.5

Table 1: Chemical Compositions (in wt%) of the A/SM Sample after Heat Treatment by XRF

The results of the Archimedes method show that the sample was highly consolidated with a relative density of 99.2%. As shown in Figure 6, significantly fewer internal defects, such as porosities and voids, can be found in the A/SM sample than in the one fabricated by AIM. It is believed that in Figure 6 (a) , the voids are attributed to the air trapped in the casting (air bubbles) while the porosities

are due to impurities pulled out during the sample polishing process. The voids shown in Figure 6 (b) are considered from the trapping of the protective gas into the melt pool during the A/SM process.

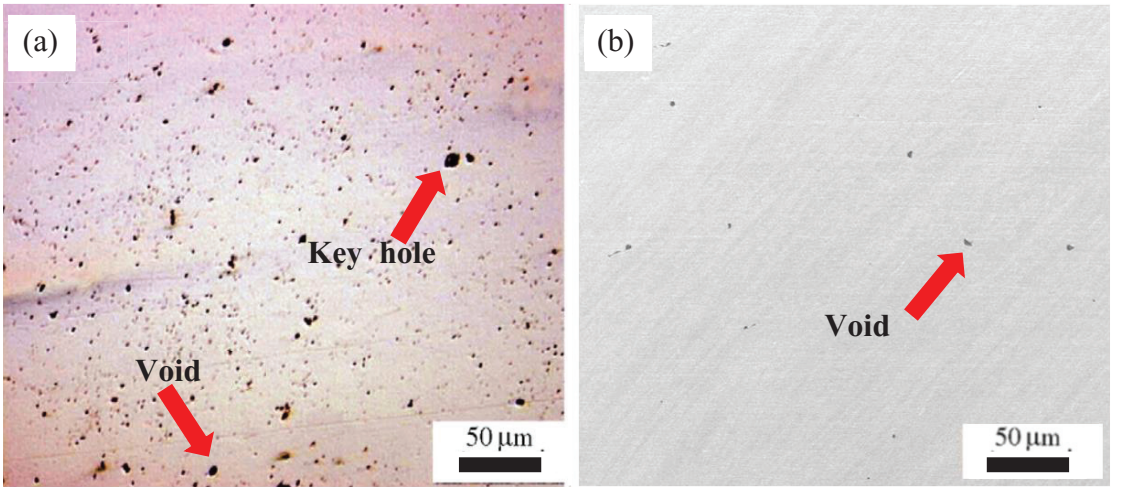

Figure 6: Cross-sectional observations of (a) AIM casting sample (Hoseini et al., 2008) and (b) A/SM sample.

4.1 Surface and microstructure characterization

Figure 7 gives a comparison of the surface morphology between the samples from the simplex SLM and hybrid A/SM processes. The simplex SLM surface was rough with unmelted powders. On the other hand, the A/SM surface was smooth even after the heat treatment. Because of the stair effect during the powder melting process, surface quality was inferior, which was one of the major drawbacks in the simplex AM process. Furthermore, the unmelted powders tended to adhere to the edge of the melting pool, resulting in a higher surface roughness, as shown in Figure 7(a). However, the subsequent subtractive milling process can effectively compensate for the dimensional and geometric inaccuracies resulted from the powder melting process as in Figure 7(b).

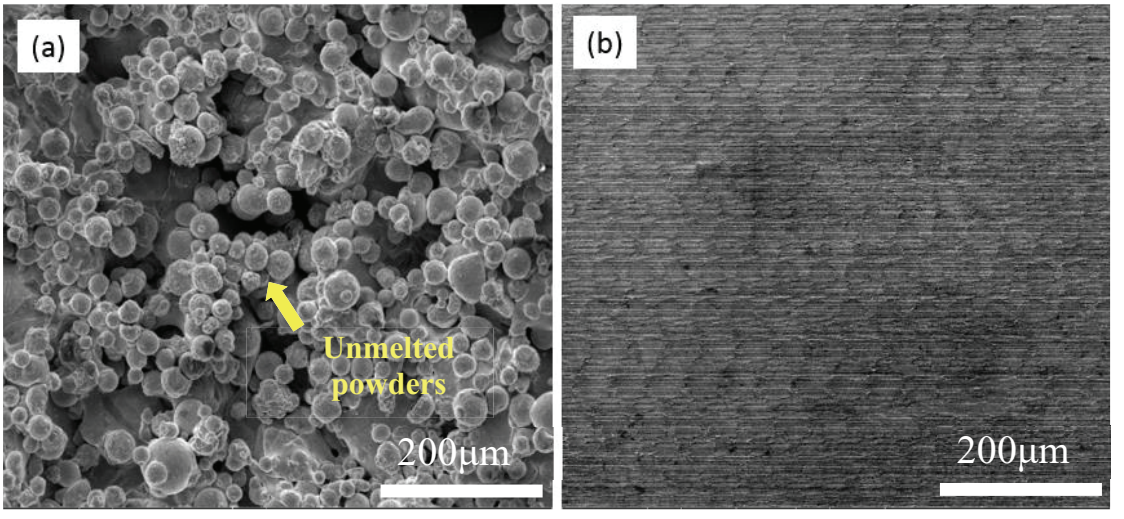

Figure 7: Surface morphology of the samples fabricated by (a) SLM and (b) A/SM processes.

Figure 8 shows an SEM image of the cross sections of the sample with both A/SM surface (left) and simplex AM surface (right). According to a study on the surface condition and the mechanical properties of a part produced by an SLM process, when a part undergoes a cyclic loading condition, microcracks are usually generated in the rough AM surface, which can be stress raisers and promote the crack initiation. The subsequent machining process is thus an important step towards improving the fatigue resistance and ductility of the part significantly (Kasperovich et al., 2015).

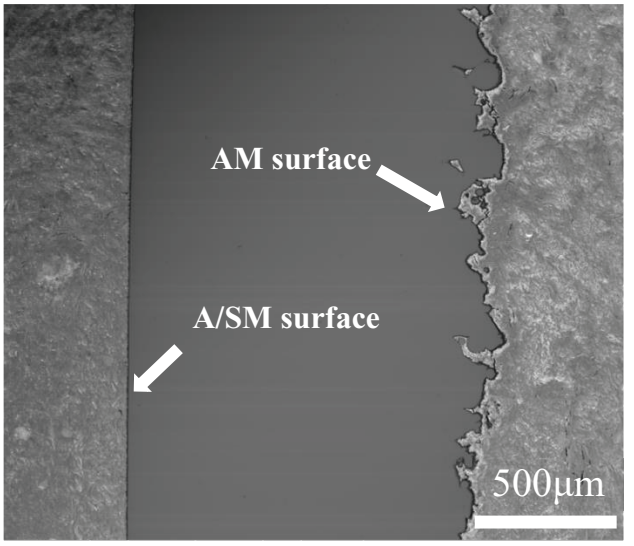

Figure 8: Cross sectional view of the A/SM and simplex AM surfaces.

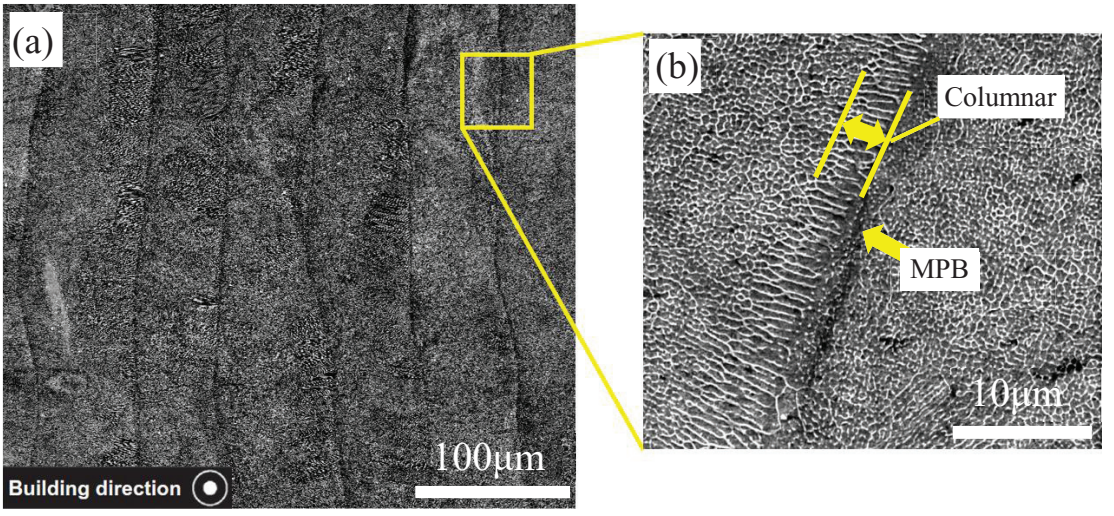

Figure 9: Microstructure of the 18Ni maraging steel sample on horizontal section (a) lower magnification; (b) higher magnification.

Figure 9 gives the SEM micrographs of the A/SM fabricated maraging sample from the top surface. The individual scan tracks and their scan direction can be recognized. The micrographs were taken from approximately the central area of the sample (in the building direction) to minimize any potential influence of the substrate or the top surface. Additionally, under the observations at high magnifications (Figure 9 (b)), bundles of very fine solidification cells are observed which are considered due to a higher cooling rate during the solidification process. However, through the observation of the boundary between the traces, a fine columnar grain structure is formed that is perpendicular to the melt pool boundary (MPB). The observations show the transition from planar to cellular solidification at the melt pool boundary. The columnar grains grow mainly along the direction of the fastest heat transfer, i.e., perpendicular to the laser track direction. The yellow lines indicate the planar zone of which the width is about 5-8 μm. This columnar grain zone is similar to the heat-affected zone in a welding process. The heat transfer and the solidification of the melted pools of the newly generated trace release a certain amount of heat, leading to the recrystallization and growth of the solidified metal in the previous trace near the melt pool boundary (Wen et al., 2014).

In Figure 10, boundaries of the tracks are made visible by etching, the cross sections of the melted tracks can be seen in the form of a series of arcs induced by the Gaussian distribution of the laser energy. Obviously, all the melted tracks are closely stacked to form a good metallurgical bonding between two neighboring layers. Similar structures have been noted in the SLM fabrication of 316L and Inconel 625 by other researchers (Jinhui et al., 2010, Yadroitsev et al., 2007).

Nevertheless, the grains consisting of fine cellular and dendritic structures are mostly unconfined to the melt pool borders, which means the orientation of some solidification dendrites do not change at the track interface as indicated by the yellow arrows in Figure 10. This is expected, since every layer is partially re-melted upon the deposition of the subsequent layer, thereby alleviating the need for repeated nucleation (Jägle et al., 2014). Besides that, it is worth noting that the growth direction of the dendrites is nearly in parallel to the Z-direction. In the process of cooling solidification of the liquid metal, heat mostly dissipates in the negative Z-direction due to the cooling effect caused by the substrate. Under the action of the highest temperature gradient and solidification rate in the Z-direction, grains grow with the directional selection to form dendrites. So the orientation of some dendrites was 'inherited' layer by layer from the substrate to the final surface of the sample along the building direction.

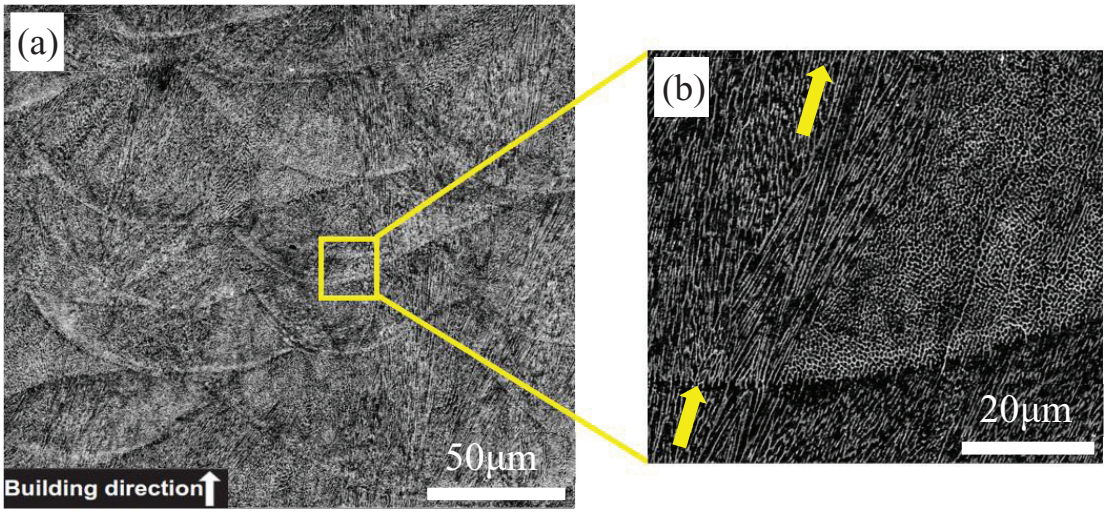

Figure 10: Microstructure of the 18Ni maraging steel sample on cross section. (a) lower magnification; (b) higher magnification.

4.2 Hardness measurement

Heat treatment was conducted on the fabricated mold sample in aging for three hours at a temperature of 500°C. The hardness of the sample was measured in different directions and compared with that of the samples fabricated by the simplex SLM and wrought maraging steels, as shown in Figure 11. It is observed that there is not much difference in hardness between the top and side surfaces of the sample. A hardness of 56.2 HRC was achieved in the top surface of the sample, which means an increase of about 16HRC compared to the SLM part without heat treatment (Kempen et al., 2011) and about 21HRC compared to the hardness of a wrought maraging steel (Latrobe specialty steel company, 2009).

In the conventionally formed maraging steels, high hardness is mainly attributed to the precipitation of the densely distributed fine intermetallic precipitates in a martensitic structure, which strengthens the alloys through the Orowan-type mechanism. Typically, this kind of microstructure is adjusted by a two-step heat-treatment process which consists of a solution annealing process to produce a complete martensitic structure, and a subsequent aging process at intermediate temperatures to cause precipitation hardening (An et al., 2012). However, in the A/SM fabrication of a maraging steel part, only aging heat treatment is needed, which may be attributed to the high cooling rate for martensite formation. Further investigations are necessary on the phase transformation during the A/SM and heat-treatment processes.

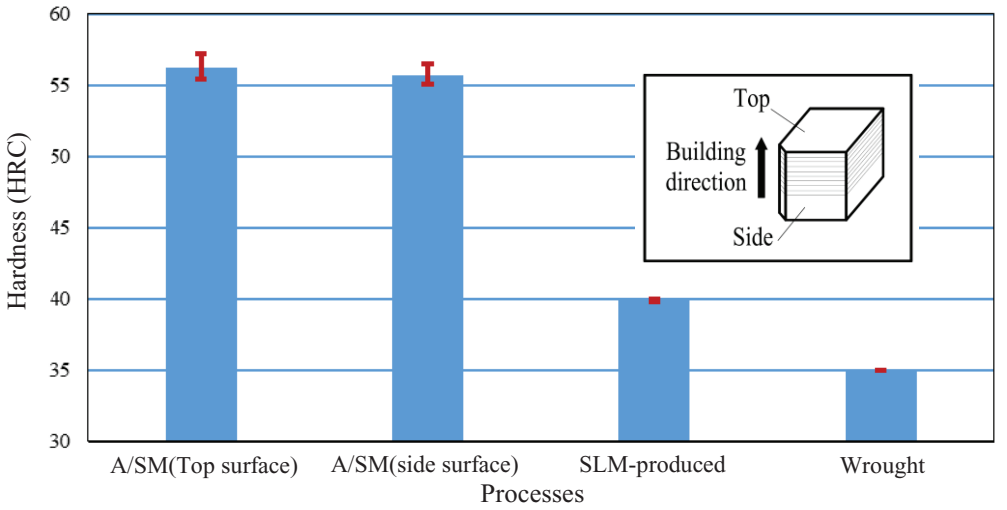

Figure 11: Hardness of the maraging samples prepared in different directions and processes.

4.3 Phase characterization

The superior properties of the maraging steels, i.e., good strength and toughness, are achieved by the age hardening of a ductile, low-carbon body-centered cubic (bcc) martensitic structure. Therefore, age hardening is standard for maraging steels and is aimed at forming a uniform distribution of fine nickel-rich intermetallic precipitates during the aging process of the martensite. These precipitates serve to strengthen the martensitic matrix. A detrimental side is the reversion reaction of the metastable martensite into austenite and ferrite (Handbook, A. S. M., 1991).

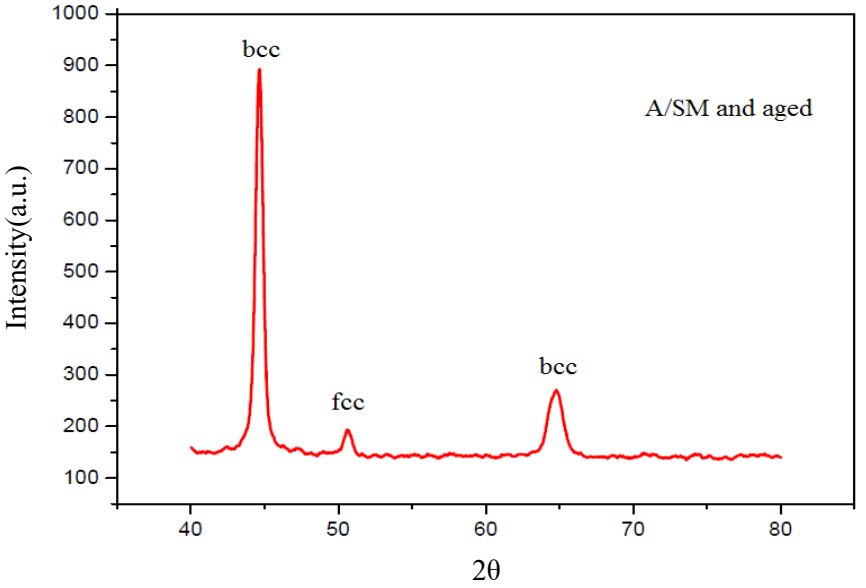

Figure 12: Results of XRD measurement after A/SM process and heat treatment.

It is necessary to identify the phase compositions of the sample due to the specialties of the A/SM process and to compare with those manufactured by the conventional methods. The result is shown in Figure 12. The main constituent phase is martensite (bcc, body cubic centered). The applied heat treatment causes an increase in the austenite phase (fcc, face cubic centered). The austenite reversion is inevitable for long aging times, because the martensite is metastable and transforms into the stable austenite. The austenite reversion is promoted by the release of Ni into the Fe matrix which accompanies the transformation from Ni_3(Mo, Ti) to the more stable Fe_2Mo precipitates (Pardal et al., 2006).

5 Conclusions

This study investigates a novel method for additive and subtractive manufacturing of metallic parts. The method can manufacture maraging steel molds with better geometric and dimensional accuracies as well as surface quality than that of the simplex SLM. The mold sample made by the method has a high relative density of 99.2% and a microstructure of fine cellular and epitaxial dendrites along the building direction. The hardness of A/SM sample is much higher than that of the simplex SLM and the wrought maraging steels. Meanwhile, it does not show large hardness variation on its top and side surfaces although its microstructure differs significantly in different directions.

References

Aziz, M. S. A., Ueda, T., Furumoto, T., Abe, S., Hosokawa, A., & Yassin, A. Study on Machinability of Laser Sintered Materials Fabricated By Layered Manufacturing System: Influence of Different Hardness of Sintered Materials. *Procedia CIRP*, 2012; 4: 79-83.

An, J., Meng, F., Lv, X., Liu, H., Gao, X., Wang, Y., & Lu, Y. Improvement of mechanical properties of stainless maraging steel laser weldments by post-weld ageing treatments. *Materials & Design*, 2012; 40: 276-284.

Choi, D. S., Lee, S. H., Shin, B. S., Whang, K. H., Song, Y. A., Park, S. H., & Jee, H. S. Development of a direct metal freeform fabrication technique using CO_2 laser welding and milling technology. *Journal of Materials Processing Technology*, 2001; 113(1): 273-279.

Cubberly, W. H., Masseria, V., & Kirkpatrick, C. W. *ASM metals handbook*, 1979.

Fessler, J. R., Merz, R., Nickel, A. H., Prinz, F. B., & Weiss, L. E. Laser deposition of metals for shape deposition manufacturing. In: *Proceedings of the solid freeform fabrication symposium*, 1996, pp. 117-124.

Freyer, C., & Klocke, F. Fast manufacture of high strength tools from steel using CMB. In: *Proceedings of SME Conference Rapid Prototyping and Manufacturing*, 2001, pp.14-17.

Griffith, M. L., Keicher, D. M., Atwood, C. L., Romero, J. A., Smugeresky, J. E., Harwell, L. D., & Greene, D. L. Free form fabrication of metallic components using laser engineered net shaping (LENS). In: *Proceedings of the Solid Freeform Fabrication Symposium*, 1996, pp.125-131.

Hoseini, S. R. E., Arabi, H., & Razavizadeh, H. Improvement in mechanical properties of C300 maraging steel by application of VAR process. *Vacuum*, 2008; 82(5): 521-528.

Handbook, A. S. M. *Volume 4 Heat Treating, ASM International, The Materials Information Company,* United States of America, pp. 528-548, 1991, ISBN 0-87170-379-3.

Jeng, J. Y., & Lin, M. C. Mold fabrication and modification using hybrid processes of selective laser cladding and milling. *Journal of Materials Processing Technology*, 2001; 110(1): 98-103.

Jägle, E. A., Choi, P. P., Van Humbeeck, J., & Raabe, D. Precipitation and austenite reversion behavior of a maraging steel produced by selective laser melting. *Journal of Materials Research*, 2014; 29(17): 2072-2079.

Jinhui, L., Ruidi, L., Wenxian, Z., Liding, F., & Huashan, Y. Study on formation of surface and microstructure of stainless steel part produced by selective laser melting. *Materials Science and Technology*, 2010; 26(10): 1259-1264.

Kempen, K., Yasa, E., Thijs, L., Kruth, J. P., & Van Humbeeck, J. Microstructure and mechanical properties of Selective Laser Melted 18Ni-300 steel. *Physics Procedia*, 2011; 12: 255-263.

Khaing, M. W., Fuh, J. Y. H., & Lu, L. Direct metal laser sintering for rapid tooling: processing and characterisation of EOS parts. *Journal of Materials Processing Technology* 2001; 113(1): 269-272.

Kruth, J. P., Leu, M. C., & Nakagawa, T. Progress in additive manufacturing and rapid prototyping. *CIRP Annals-Manufacturing Technology*, 1998; 47(2): 525-540.

Karunakaran, K. P., Suryakumar, S., Pushpa, V., & Akula, S. Low cost integration of additive and subtractive processes for hybrid layered manufacturing. *Robotics and Computer-Integrated Manufacturing,* 2010; 26(5): 490-499.

Kruth, J. P., Froyen, L., Van Vaerenbergh, J., Mercelis, P., Rombouts, M., & Lauwers, B. Selective laser melting of iron-based powder. *Journal of Materials Processing Technology*, 2004; 149(1): 616-622.

Kasperovich, G., & Hausmann, J. Improvement of fatigue resistance and ductility of TiAl6V4 processed by selective laser melting. *Journal of Materials Processing Technology*, 2015; 220: 202-214.

Lorenz, K. A., Jones, J. B., Wimpenny, D. I., & Jackson, M. R. A review of hybrid manufacturing. In: *Solid Freeform Fabrication Conference Proceedings*, 2015, Vol. 53.

Lewis, G., Milewski, J., Thoma, D., & Nemec, R. Properties of near-net shape metallic components made by the directed light fabrication process. In: *Proceedings of the Solid Freeform Fabrication Symposium*, 1997, pp.513-520.

Latrobe specialty steel company: *Marvac 300 vim-var data sheet, technical report*, 2009.

Masood, S. H. Intelligent rapid prototyping with fused deposition modelling. Rapid Prototyping Journal 1996; 2(1): 24-33.

Murr, L. E., Gaytan, S. M., Ramirez, D. A., Martinez, E., Hernandez, J., Amato, K. N., ... & Wicker, R. B. Metal fabrication by additive manufacturing using laser and electron beam melting technologies. *Journal of Materials Science & Technology*, 2012; 28(1): 1-14.

Pardal, J. M., Tavares, S. S. M., Fonseca, M. C., Abreu, H. F. G., & Silva, J. J. M. Study of the austenite quantification by X-ray diffraction in the 18Ni-Co-Mo-Ti maraging 300 steel. *Journal of materials science*, 2006; 41(8): 2301-2307.

Rombouts, M., Kruth, J. P., Froyen, L., & Mercelis, P. Fundamentals of selective laser melting of alloyed steel powders. *CIRP Annals-Manufacturing Technology* 2006; 55(1): 187-192.

Song, Y. A., Park, S., Choi, D., & Jee, H. 3D welding and milling: Part I–a direct approach for freeform fabrication of metallic prototypes. *International Journal of Machine Tools and Manufacture*, 2005; 45(9): 1057-1062.

Song, Y. A., Park, S., & Chae, S. W. 3D welding and milling: part II—optimization of the 3D welding process using an experimental design approach. *International Journal of Machine Tools and Manufacture*, 2005; 45(9): 1063-1069.

Wen, S., Li, S., Wei, Q., Yan, C., Zhang, S., & Shi, Y. Effect of molten pool boundaries on the mechanical properties of selective laser melting parts. *Journal of Materials Processing Technology*, 2014; 214(11): 2660-2667.

Xiong, X., Zhang, H., Wang, G., & Wang, G. Hybrid plasma deposition and milling for an aeroengine double helix integral impeller made of superalloy. *Robotics and Computer-Integrated Manufacturing*, 2010; 26(4): 291-295.

Yadroitsev, I., Thivillon, L., Bertrand, P., & Smurov, I. Strategy of manufacturing components with designed internal structure by selective laser melting of metallic powder. *Applied Surface Science*, 2007; 254(4): 980-983.